buildings

MDPI

Article

Optimization of Tuned Liquid Damper Including Different Liquids for Lateral Displacement Control of Single and Multi-Story Structures

Ayla Ocak [1], Gebrail Bekdaş [1,*], Sinan Melih Nigdeli [1], Sanghun Kim [2] and Zong Woo Geem [3,*]

[1] Department of Civil Engineering, İstanbul University-Cerrahpaşa, İstanbul 34320, Turkey; aylaocak@outlook.com (A.O.); melihnig@iuc.edu.tr (S.M.N.)
[2] Department of Civil and Environmental Engineering, Temple University, Philadelphia, PA 19122, USA; sanghun.kim@temple.edu
[3] Department of Smart City & Energy, Gachon University, Seongnam 13120, Korea
* Correspondence: bekdas@iuc.edu.tr (G.B.); geem@gachon.ac.kr (Z.W.G.)

Abstract: This study focuses on tuned liquid dampers (TLDs) using liquids with different characteristics optimized with the adaptive harmony search algorithm (AHS). TLDs utilize the characteristic features of the liquid to absorb the dynamic forces entering the structure and benefit from the sloshing movement and the spring stiffness created by the liquid mass. TLDs have been optimized to investigate the effect of liquid characteristics on the control by analyzing various liquids. For optimization, the memory consideration ratio (HMCR) and fret width (FW) values were adapted from the classical harmony search (HS) algorithm parameters. The TLDs were used on three types of structure models, such as single-story, 10, and 40 stories. The contribution of the liquid characteristics to the damping performance was investigated by optimizing the minimum displacement under seismic excitation. According to the results, it was understood that the liquid density and kinematic viscosity do not affect single-story structures alone. However, two characteristic features should be evaluated together. As the structure mass increases, the viscosity and density become more prominent.

Keywords: harmony search; adaptive harmony search; tuned liquid damper; structural control; optimization

Citation: Ocak, A.; Bekdaş, G.; Nigdeli, S.M.; Kim, S.; Geem, Z.W. Optimization of Tuned Liquid Damper Including Different Liquids for Lateral Displacement Control of Single and Multi-Story Structures. *Buildings* **2022**, *12*, 377. https://doi.org/10.3390/buildings12030377

Academic Editor: Davor Stanko

Received: 7 March 2022
Accepted: 16 March 2022
Published: 18 March 2022

1. Introduction

Passive control systems are low-cost, easy to maintain and repair energy-saving systems that adopt Newton's principle of conservation of energy and use the energy they collect in damping without losing it. These systems include a mass and spring model to perform damping by acting depending on the displacement or velocity. Tuned liquid dampers (TLDs) are a displacement-dependent passive control system connected to the structure by a liquid mass and spring. They use the agitation energy of the liquid. The rate of circulation of the tank liquid in the system is sloshing by considering the natural period of the structure. These dampers provide control against the seismic loading by moving in the opposite direction to the movement of the structure. Abramson et al. described the sloshing in a cylindrical tank by examining and creating a model in which the liquids are not fully sloshing but some liquid remains motionless [1,2]. This liquid, which remains inactive and passive, is considered to move with the damper tank. In this way, TLDs can treat the movement of the active liquid as two degrees of freedom, assuming it is independent of the tank.

In the beginning, the main control parameters of liquid dampers are tank geometry, liquid mass, and frequency. Although it is recommended in the literature that the mass of TLD can be taken between 1% and 4%, in principle, a mass ratio of 5% is recommended for tuned mass dampers (TMDs) as a passive damper with the same characteristics [3–6]. As with all passive dampers, the mass was the main control parameter sloshing in tuned liquid

damper devices. To make the mass-related TLD and its derivatives more efficient, inerter devices that slosh the amount of the effect of the mass are added, and the effect of the mass on damping becomes more controllable. When Wang et al. examined the new tuned liquid column damper inerter device (TLCDI) under white noise and seismic excitations, it was found that it was more efficient and robust against frequency ratio distortion than the conventional tuned liquid column damper (TLCD). Di Matteo et al. also confirmed the efficiency of adding an inerter device by using the TLCDI device in the control against seismic base excitations and observed that it transforms the TLDs into a lighter control device [7,8]. Wang et al., in their study of multiple tuned liquid column damper inerter devices (MTLCDI), found that they can outperform a single TLCDI device [9]. TLDs are named according to the bottom geometry of the tank. While they generally have rectangular or circular base geometry, there have also been studies on TLDs with conical designed geometry in the literature [10,11]. In research on tank geometry, flat and curved bottom geometries were compared, and TLDs with inclined tank geometry were found to have low liquid contents, etc. It was found that flat-bottomed TLDs were more efficient in terms of durability [12,13]. Fujino et al. developed a design element for TLDs through a study of TLD tank sizes [14]. Regardless of the bottom geometry of the tank, a ratio was proposed between the long bottom edge where the liquid is shaken more easily and the maximum liquid height that the tank will reach. According to this ratio, the ratio of the maximum height of the tank (the height that the liquid should not exceed) to the effective liquid length at the bottom size should be greater than 15%. The proposed ratio established a TLD design standard by reducing the possibility of exceeding the maximum liquid height created by sloshing in a TLD design. Since liquid dampers benefit from the displacement of the mass, the circulating time of the agitated liquid in the system directly affects the control. The period selection of TLD is tuned according to the natural period of the structure, as in other mass dampers. Balendra et al. stated that, to prevent wind vibrations of a tower, the TLCD device can provide the best performance by tuning the frequency of the damper at the frequency of the structure [15].

In damping, the characteristic properties of the liquid affect the properties like the energy of sloshing, damping rate, and period. The viscosity and density of the selected liquid form the basic liquid characteristics that control the damping. Apart from TLD optimization studies with several liquids on the damping effect of the kinematic viscosity and density of the liquid, some studies included density tuned by adding various liquid mixtures and additional balls. Ocak et al., using metaheuristic algorithms, optimized TLDs attached to a single-story structure using three different densities and viscosities of water, oil, and glycerin liquids and obtained water as the optimum liquid [16]. In the study of the tuned liquid column ball damper (TLCBD) with mixtures of different densities and balls, a better control performance was obtained with liquid and high-density balls [17]. Shah et al. determined that the tuned liquid column ball spring damper (TLCBSD) and its modified type, which was developed by connecting the ball placed in the liquid to the tank with the help of a spring [18], could be better than TLCBD. Hitchcock et al., on unidirectional liquid column vibration absorbers (LCVA), observed that the damping rate depends on the Reynolds number, which is the ratio of the inertial forces of the liquid to the viscosity forces [19]. Some studies suggested that the use of denser TLCD fluid in energy dissipation increased the damper performance [20–22]. Various studies have been carried out to control the characteristic properties of liquids. It has been stated that TLDs containing magnetorheological liquids could provide a better damping capacity [23,24]. To increase the control performance of TLDs, magnetorheological liquids (MR liquids) were used in TLD tanks to tube the liquid viscosity. MR liquids directly affect the mechanical properties of sloshing, such as the viscosity and damping ratio, by using the magnetic field created by the magnetic parts in it to tune the viscosity. Although it is among the advantages of these liquids to tune the viscosity at constant liquid densities, it is a disadvantage that they need an additional additive to prevent the precipitation of magnetic particles in the composite liquid and, therefore, a new parameter that must be kept under control.

The damping capacity of TLDs is tuned with the help of the liquid mass and spring stiffness. The total liquid mass of the tank and the spring stiffness depends on the liquid density and the tank geometry, as well as the damping rate parameter of the agitation, which is a variable dependent on the kinematic viscosity of the liquid. Considering this situation, it is understood that the density and kinematic viscosity are two parameters that should be evaluated together, not alone. Performing this evaluation stage with the optimization method provides more robust data for the efficiency of the control. The use of metaheuristic algorithms has become very common, because they create the most suitable mathematical models for the optimization process with the perfect nature cycle in living life and are simple and understandable. The application of metaheuristic algorithms on the optimization of TLD and its derivatives has led to successful results in the control [16,25–32]. The harmony search algorithm (HS) is a metaheuristic algorithm inspired by the best harmony search process developed by Geem et al. [33]. The HS algorithm has been supported by studies that had remarkable effects on the optimization of mass dampers in which TLDs were in the control group, as well as in various engineering problems [34–42]. Adapting the parameters of the HS algorithm has made the optimization more efficient. The classical HS algorithm includes design factors suitable for adaptation, such as the harmony memory consideration ratio (HMCR), fret width (FW), and bandwidth (bw). Improved HS adaptations obtained by adapting the algorithm have provided better results than classical optimization methods in damper calculation parameters like the frequency, damping ratio, and the mass ratio [43–47]. Studies with HS adaptations and hybrids in various engineering problems have made them stand out among the metaheuristic algorithms in their group [48–52].

The densities and viscosities of liquid used in the TLD are effective on the response of the system. In that case, the best liquid that has the best performance needs to be investigated. In previous works, generally, water-based TLDs were investigated. Although Ocak et al., [16] investigated three types of liquids in an optimum design using single degree of freedom main systems, new liquids that have extremely different characteristics need to be investigated. Additionally, the structure system controlled via a TLD must be several ones having multiple degrees to see the performance differences of liquids in different models.

In this study, a cylindrical liquid damping device tuned with various liquids was used on single-story, ten-story, and forty-story building models. Its control performance was investigated under seismic excitations. The adaptive harmony search algorithm (AHS) [53] was considered in the optimum TLD design of water-based TLDs, and this algorithm was found to be effective. For this purpose, the TLD device parameters, including liquids of different densities and viscosities, were optimized with AHS, and the performance was investigated on various types of structures, including a forty-story model that is not considered with a TLD. The optimum liquid was determined to provide the necessary conditions for a TLD to show minimum displacement under seismic excitations. The optimization process and dynamic analysis via seismic excitations were carried out with the help of MATLAB Simulink [54]. In the study, FEMA earthquake records consisting of 22 two-component earthquakes were used [55]. By comparing the effects of the density and viscosity properties of liquid types on the control, their performances in single-story, ten-story, and forty-story structures were evaluated. The relationship between the liquid characteristics and the control was investigated.

2. Materials and Methods

The design parameters of TLDs greatly affect the seismic control. The TLD parameters are optimized, resulting in a more efficient controller. In this section, information is given about the HS algorithm used in the TLD analysis with different liquids, TLD parameter formulations, damper motion equations, and the methodology of the study.

2.1. Design of TLDs and Equations of Motion

TLDs provide the seismic control with displacements created by oscillations by using the liquid mass and spring stiffness. It aims to absorb the energy by moving the tank liquid in the opposite direction to the response of the structure in the face of any dynamic load coming to the structure. In Figure 1, liquid motion versus structure motion is shown schematically.

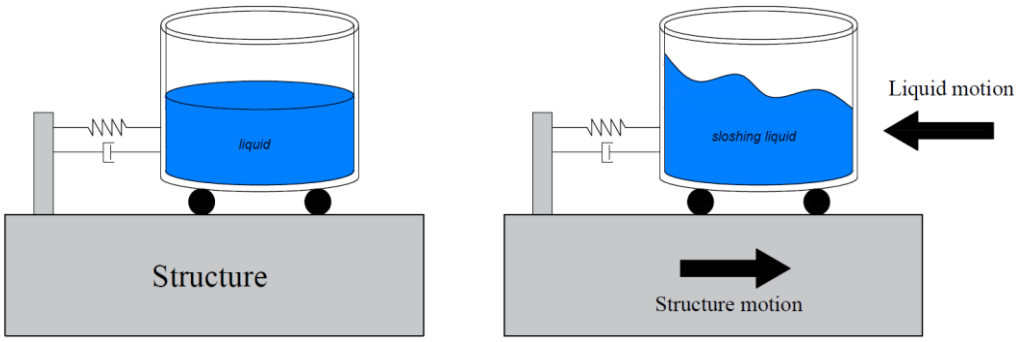

Figure 1. The structure + TLD model (**a**) static position of the system and (**b**) sloshing motion that occurs in the TLD.

Considering that tank liquid sloshing provides damping, it is seen that the first consideration for TLD design is the liquid mass. After deciding on the density of the liquid and the tank dimensions, the calculations of the liquid mass circulating in the system form the basis of the design. In the sloshing model of a cylindrical tank, which Abramson calculated based on the linear hydrodynamic theory, this liquid mass is divided into two as active and passive liquids, according to its motion capacity [1]. The liquid that expresses the moving mass in the system is called agitation fluid, while the inert mass is specified as the passive liquid that is not sloshing. Figure 2 shows the sloshing model of a cylindrical TLD with both active liquid and passive liquid.

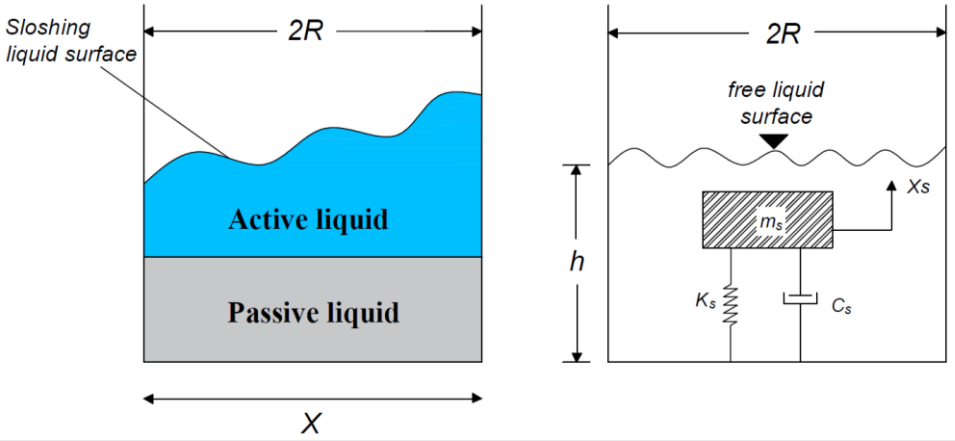

Figure 2. Cylindrical TLD sloshing model.

For a cylindrical tank, the total liquid mass (m_{st}) in the system can be calculated according to the tank dimensions and liquid density, as in Equation (1):

$$m_{st} = \pi R^2 h \rho \quad (1)$$

where h and R denote the height and radius of the cylindrical tank, respectively, and ρ denotes the density of the liquid.

The Bessel function, which is used in the calculations of wave propagation in cylindrical bodies, is used to calculate the mass and stiffness of the sloshing liquid in the system. The roots of the Bessel function give the damping ratio parameter (ξmn) [56]. The indices of this parameter represent the vibration modes of the liquid in the tangential (m) and radial (n) directions. The calculations are made according to the 1st vibration mode in all directions of the basic model of the liquid, and the damping velocity parameter value is obtained as 1.84 [56,57]. This value provides the calculation of the natural frequency and stiffness of the sloshing by calculating the lateral forces resulting from the sloshing in the tank [2,56]. The sloshing liquid mass (m_s) calculation of the system is calculated as in Equation (2):

$$m_s = m_{st} \times R \times \frac{\tanh\left(\frac{1.84h}{R}\right)}{2.2h} \tag{2}$$

The active and passive liquids, which are divided into two in the tank, act as a two degrees of freedom system. Active liquid movement denotes one freedom, while passive liquid movement with TLD denotes the other freedom. The total mass of TLD (m_{TLD}) can be chosen between 1% and 5% following the literature. The sum of the empty tank mass and passive liquid mass (m_d), which represents the second freedom, is calculated as in Equation (3):

$$m_d = m_{TLD} - m_s \tag{3}$$

The sloshing liquid stiffness (k_s) and damping coefficient (c_s) and TLD spring stiffness (k_d) and damping coefficient (c_d) calculations are shown in Equations (4)–(7), respectively. The TLD period is referred to as T_d in the equations.

$$k_s = m_{st} \times \frac{g\left\{\tanh\left(\frac{1.84h}{R}\right)\right\}^2}{1.19h} \tag{4}$$

$$c_s = \zeta_s \times 2\sqrt{m_s k_s} \tag{5}$$

$$k_d = m_d \times \left(\frac{2\pi}{T_d}\right)^2 \tag{6}$$

$$c_d = 2 \times \zeta_d \times \sqrt{m_d \times k_d} \tag{7}$$

As a result of various experimental studies, the damping rate (ζ_s) of the sloshing liquid was derived as in Equation (8) [1,56,58]. The kinematic viscosity of the fluid (ν) and the TLD damping ratio (ζ_d) are shown in Equations (8) and (9), respectively.

$$\zeta_s = 4.98 v^{\frac{1}{2}} R^{-\frac{3}{4}} g^{-\frac{1}{4}} \left[1 + \frac{0.318}{\sinh\left(\frac{1.84h}{R}\right)} \frac{1 - \frac{h}{R}}{\cosh\left(\frac{1.84h}{R}\right)}\right] \tag{8}$$

$$\zeta_d = \frac{c_d}{2m_d\sqrt{\frac{k_d}{m_d}}} \tag{9}$$

The terms belonging to the sloshing liquid in the equations are expressed with the "s" index, and the terms belonging to the TLD are expressed with the "d" index. Unindexed terms are terms that describe the properties of the structure. In its simplest form, the TLD equation of motion is as in Equation (10). The mass, stiffness, and damping coefficient matrices, which form the basic equation of motion of TLD, are given in Equations (11)–(13), respectively.

$$[M]\left\{\ddot{X}\right\} + [C]\left\{\dot{X}\right\} + [K]\{X\} = -[M]1\left\{\ddot{X}_g\right\} \tag{10}$$

$$[M] = \begin{bmatrix} m & 0 & 0 \\ 0 & m_d & 0 \\ 0 & 0 & m_s \end{bmatrix} \tag{11}$$

$$[K] = \begin{bmatrix} K + K_d & -K_d & 0 \\ -K_d & K_d + K_s & -K_s \\ 0 & -K_s & K_s \end{bmatrix} \tag{12}$$

$$[C] = \begin{bmatrix} C + C_d & -C_d & 0 \\ -C_d & C_d + C_s & -C_s \\ 0 & -C_s & C_s \end{bmatrix} \tag{13}$$

2.2. Harmony Search and Adaptive Harmony Search Algorithm

The HS algorithm is a metaheuristic algorithm developed by Geem et al., [33] inspired by the process of searching for the best-sounding harmony. This algorithm contains design factors. Parameters like the harmony memory consideration rate (HMCR) and fret width (FW) are the basic design parameters of the harmony search algorithm. The optimization process, similar to other algorithms, begins with the definition of the objective function of the problem, the design constraints, the lower and upper limit values, and the introduction of parameters like the population number to the system. The objective function in TLD design aims to obtain the minimum displacement against the vibration coming into the structure. The design lower and upper limits can be defined according to the structure applied. However, a general design constraint regarding tank dimensions should be introduced to the system at the outset. The ratio of the height and diameter of the cylindrical tank, which are given in the first section, will affect the possible solution vectors created.

For HS optimization, a random harmony vector is created within the limit values and stored for later use. This process is repeated according to the number of harmony memory sizes (HMS), allowing multiple harmony vectors to be stored in memory. The harmony vector generation process is given in Equation (14):

$$X_{new} = X_{min} + rand\ (X_{max} - X_{min})\ if\ \text{HMCR} \leq rand \tag{14}$$

Each obtained harmony vector is written into the objective function, and the data are recorded in the solution matrix. The harmony vector creation process is repeated for the number of iterations defined in the system, resulting in the formation of new solution matrices. There are two options for each new harmony vector created.

The new harmony vector can also be created with the help of Equation (15):

$$X_{new} = X_n + rand\ \text{FW}\ (X_{max} - X_{min})\ if\ \text{HMCR} > rand \tag{15}$$

In the stage of deciding which of the two given equations to choose to create the harmony vector, the harmony memory consideration ratio takes on the task of choosing. New harmony vectors are created with the help of Equation (14) when a randomly selected value between 0 and 1 is less than the HMCR value and Equation (15) when it is greater than or equal to the value of the HMCR. The solution matrices obtained with the new vectors are compared with the previous solutions, the best one is decided, and the solutions are updated. When all iterations are completed, the best harmony is achieved.

The AHS algorithm is obtained by adapting the harmony memory consideration rate (HMCR) and fret width (FW) parameters. First, these two parameters are given an initial value. Then, this initial value gradually decreases, looking for the optimum solution until it reaches zero. The equations for the HMCR and FW parameters are Equations (16) and (17):

$$\text{HMCR} = \text{HMCR}_{in}\left(1 + \frac{t}{mt}\right) \tag{16}$$

$$\text{FW} = \text{FW}_{in}\left(1 - \frac{t}{mt}\right) \tag{17}$$

In the equations, the initial values $HMCR_{in}$ and FW_{in} are indicated by the iteration number t and the maximum iteration number mt.

AHS was selected in the optimization, since it has been proven as an effective algorithm in the optimum design of TLD to have water as the liquid [53].

3. Numerical Examples

The structural models were created by placing TLDs containing liquids of various densities and viscosities on single-story, ten-story, and forty-story structures. FEMA earthquake records were used in simulations for each model, which were composed with MATLAB Simulink. The list of earthquake records used is shown in Table 1 [55].

Table 1. FEMA earthquake records list.

Earthquake Number	Date	Earthquake Name	Component 1	Component 2
1	1994	Northridge	NORTHR/MUL009	NORTHR/MUL279
2	1994	Northridge	NORTHR/LOS000	NORTHR/LA270
3	1999	Duzce, Turkey	DUZCE/BOL0000	DUZCE/BOL090
4	1999	Hector Mine	HECTOR/HEC000	HECTOR/HEC090
5	1979	Imperial Valley	IMPVALL/H-DLT262	IMPVALL/H-DLT352
6	1979	Imperial Valley	IMPVALL/H-E11140	IMPVALL/H-E11230
7	1995	Kobe, Japan	KOBE/NIS000	KOBE/NIS090
8	1995	Kobe, Japan	KOBE/SHI000	KOBE/SHI090
9	1999	Kocaeli, Turkey	KOCAELI/DZC180	KOCAELI/DZC270
10	1999	Kocaeli, Turkey	KOCAELI/ARC000	KOCAELI/ARC090
11	1992	Landers	LANDERS/PLACE270	LANDERS/YER360
12	1992	Landers	LANDERS/CLW-LN	LANDERS/CLW-TR
13	1989	Loma Prieta	LOMAP/CAP000	LOMAP/CAP090
14	1989	Loma Prieta	LOMAP/G03000	LOMAP/G03090
15	1990	Manjil, Iran	MANJIL/ABBAR–L	MANJIL/ABBAR–T
16	1987	Superstition Hills	SUPERST/B-ICC000	SUPERST/B-ICC090
17	1987	Superstition Hills	SUPERST/B-POE270	SUPERST/B-POE360
18	1992	Cape Mendocino	CAPEMEND/RIO270	CAPEMEND/RIO360
19	1999	Chi-Chi, Taiwan	CHICHI/CHY101-E	CHICHI/CHY101-N
20	1999	Chi-Chi, Taiwan	CHICHI/TCU045-E	CHICHI/TCU045-N
21	1971	San Fernando	SFERN/PEL090	SFERN/PEL180
22	1976	Friuli, Italy	FRIULI/A-TMZ000	FRIULI/A-TMZ270

Acetone, mercury, seawater, chloroform, and propanol liquids were used for the TLD tank. These liquids were tested in the study, because their densities and viscosities have differences suitable for comparison and can be easily obtained in various fields, like the health sector and the chemical industry. The density and viscosity values of the liquids used in the study, measured at a constant temperature, are shown in Table 2 [59–63].

Table 2. TLD liquid properties.

Liquid	Dynamic Viscosity (Pa·s)	Temperature (°C)	Kinematic Viscosity (m^2/s)	Density (kg/m^3)
Chloroform	0.58×10^{-3}	20	3.92×10^{-7}	1480.3
Acetone	0.306×10^{-3}	25	3.90×10^{-7}	784.89
Propanol	1.945×10^{-3}	25	2.43×10^{-6}	799.60
Mercury	1.57×10^{-3}	20	1.15×10^{-7}	13,600
Sea water	1.20×10^{-3}	15.6	1.17×10^{-6}	1030

Among the TLD design parameters, the height and radius of the cylindrical tank, TLD period, and damping ratio were optimized with the AHS algorithm. All design constraints and optimization parameters are shown in Table 3.

Table 3. TLD and optimization design parameters.

Explanation	Design Parameter
TLD mass	5% of the mass of the structure
Max Height	10 m
Minimum Height	0.1 m
Max Radius	10 m
Minimum Radius	0.1 m
TLD Period	$0.5 \sim 1.5 \times$ Structure Period
The ratio of height to radius	$\frac{h}{2R} > 0.15$
Damping Ratio	1~50%
Stroke capacity	$(\lvert X_d - X \rvert)_{\text{with TLD}} / (\lvert X \rvert)_{\text{without TLD}} \leq \text{stmax}$
Population Number	10
İteration Number	1000
Fret Width initial	0.05
Harmony Memory Consideration Rate initial	0.5

3.1. Single-Story Structure

For the single-story structure model, a structured story mass of 100 tons was used. The period of the structure was taken as 1 s, and the stiffness and damping coefficient values were calculated as 3.95 MN/m and 0.06 MNs/m. The TLD + structure model is designed with three degrees of freedom (3DOF), the sloshing liquid, TLD, and structure, as seen in Figure 3.

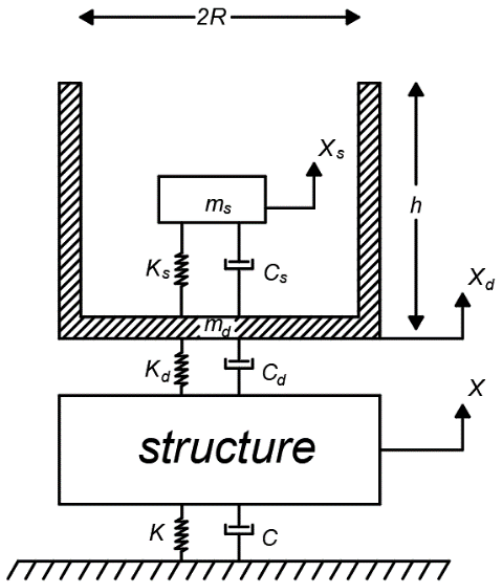

Figure 3. Cylindrical TLD + single-story structure model.

Under seismic excitations, the single-story building model was optimized with the AHS algorithm. The optimized TLD tank dimensions, period, and damping ratio are given in Table 4.

Table 4. Optimum results for all TLD liquids in the single-story structure.

Variables	Optimized Values				
	TLD				
	Chloroform	**Acetone**	**Propanol**	**Mercury**	**Seawater**
T_d (s)	1.0188	0.9454	1.0613	0.9251	1.0829
ζ_d	0.1473	0.0810	0.2336	0.0637	0.2402
R (m)	0.2947	0.5418	0.2784	0.3225	0.2395
h (m)	1.4482	2.2884	9.3378	0.1531	6.2101

In the analysis made for all liquids with optimized TLD parameters, the critical earthquake occurred in Duzce, Turkey in the FEMA records and is named DUZCE/BOL090. The maximum displacement and total acceleration values obtained from the critical seismic analysis are shown in Table 5. In addition, the results of the analysis including water optimized via AHS optimization on a single-story structure are added to the table [53].

Table 5. TLD + single-story building model critical earthquake analysis results.

Liquid	Structure with TLD		Structure without TLD	
	Displacement (m)	**Total Acceleration (m/s^2)**	**Displacement (m)**	**Total Acceleration (m/s^2)**
Acetone	0.2343740	9.0757597	0.2873419	11.4077630
Mercury	0.2358324	9.3099176		
Chloroform	0.2390329	9.3747324		
Water	0.2446071	9.5648807		
Propanol	0.2467634	9.6208562		
Seawater	0.2472287	9.6666351		

The displacement–time and total acceleration–time graphs obtained from the critical seismic analysis of acetone, mercury, chloroform, propanol, and seawater liquids used in TLD design are shown in Figures 4–8, respectively.

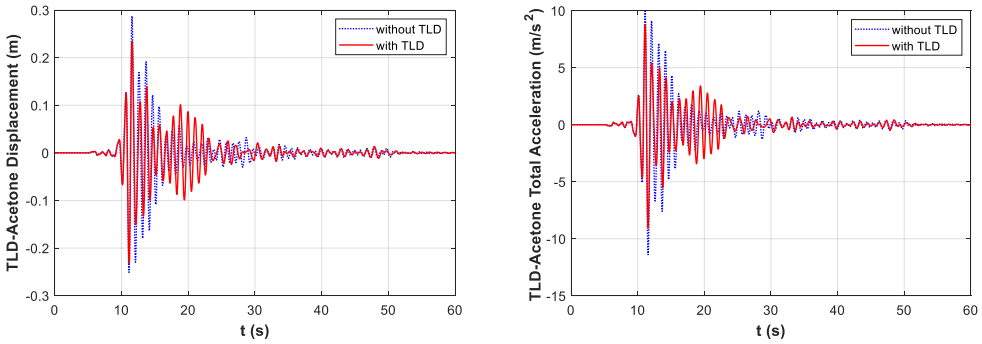

Figure 4. AHS optimization of the single-story structure displacement–time and total acceleration–time graphs in the DUZCE/BOL090 earthquake record for TLD–acetone.

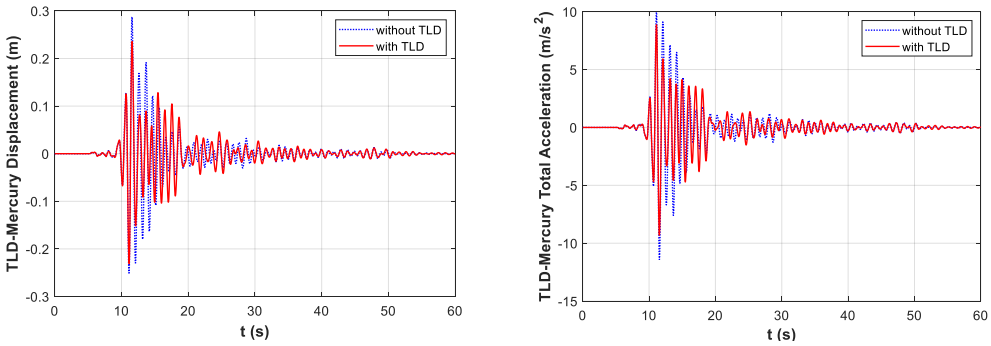

Figure 5. AHS optimization of the single-story structure displacement–time and total acceleration–time graphs in the DUZCE/BOL090 earthquake record for TLD–mercury.

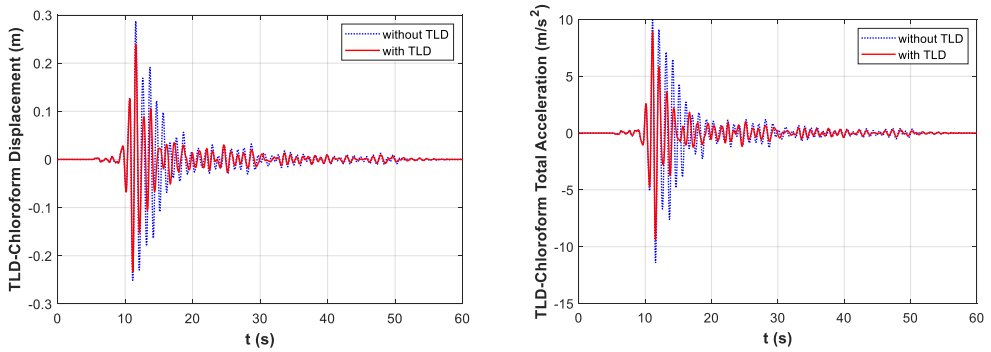

Figure 6. AHS optimization of the single-story structure displacement–time and total acceleration–time graphs in the DUZCE/BOL090 earthquake record for TLD–chloroform.

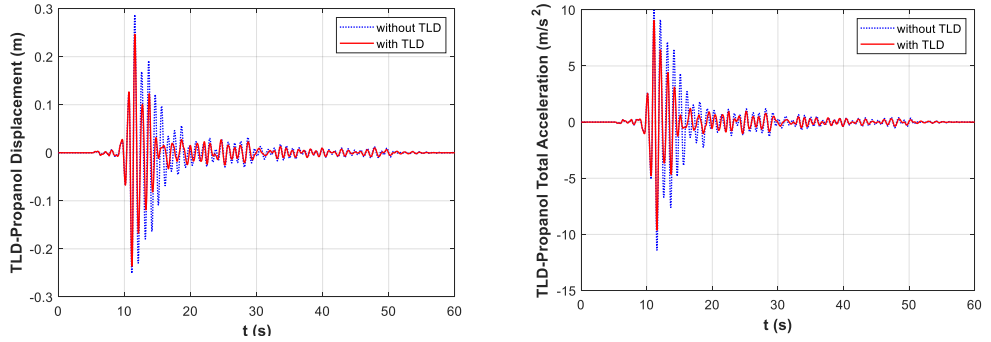

Figure 7. AHS optimization of the single-story structure displacement–time and total acceleration–time graphs in the DUZCE/BOL090 earthquake record for TLD–propanol.

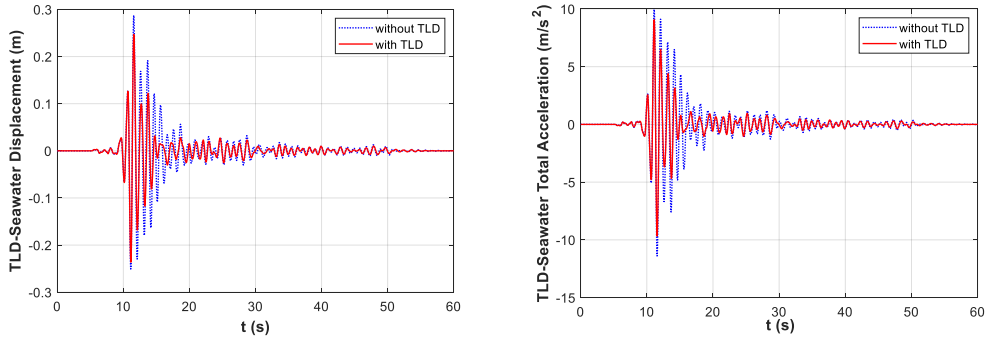

Figure 8. AHS optimization of the single-story structure displacement–time and total acceleration–time graphs in the DUZCE/BOL090 earthquake record for TLD–seawater.

The robustness of the TLD was also tested for the cases of the single-story structure. To consider the variable loading of the structure, the different masses of the structure for the same optimum TLD parameters were checked. In Table 6, the robustness of the optimum TLD for the single-story structure was investigated by changing the mass of the structure up to ±25% uncertainty. As seen from the results, the optimum TLD parameters were also effective for mass uncertainty, although the performance loss may be observed for the increase of the mass due to the reduction of mass ratio of the TLD and structure.

3.2. Ten-Story Structure

For the ten-story structure model, a building mass of 360 tons on each floor was used. The stiffness and damping coefficient values of the structure were taken as 650 MN/m and 6.2 MNs/m [64]. A 12-degrees-of-freedom (12DOF) model was created, considering the TLD liquid and the movement of the tank two freedoms and the movement of the ten-story 10 freedoms. The TLD + structure model used for the ten-story structure is shown in Figure 9.

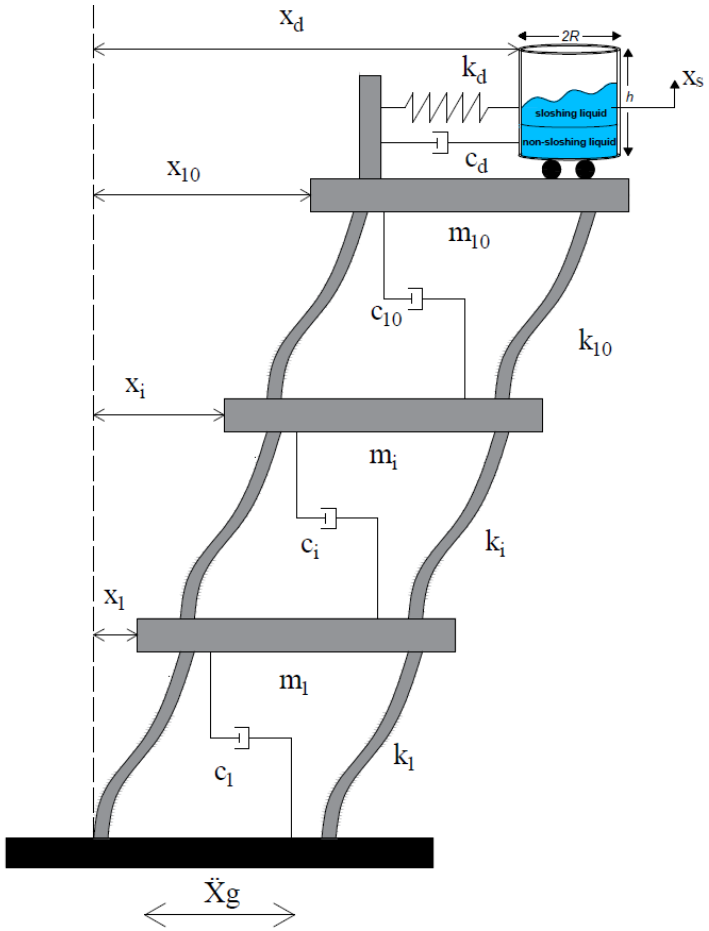

Figure 9. Cylindrical TLD plus 10-story structure model.

Table 6. The performance of the optimum TLD for the uncertainty of the mass of the single-story structure.

Structure Mass (Ton)	Without TLD Structure		TLD–Acetone		With TLD–Mercury		With TLD–Chloroform		With TLD–Propanol		With TLD–Seawater	
	Displacement (m)	Total Acceleration (m/s^2)	Displacement (m)	Total Acceleration (m/s^2)	Displacement (m)	Total Acceleration (m/s^2)	Displacement (m)	Total Acceleration (m/s^2)	Displacement (m)	Total Acceleration (m/s^2)	Displacement (m)	Total Acceleration (m/s^2)
75	0.2467190	13.0798250	0.2016451	10.5720449	0.2040501	10.8828848	0.2049643	10.8633207	0.2130885	11.1656552	0.2134193	11.2102898
80	0.2610085	12.9673247	0.2121752	10.4000571	0.2147651	10.7101163	0.2161374	10.7134861	0.2243689	11.0040281	0.2247637	11.0509856
85	0.2719087	12.7072278	0.2208049	10.1468190	0.2233240	10.4448977	0.2251804	10.4687604	0.2333662	10.7471630	0.2338051	10.7952535
90	0.2797414	12.3429855	0.2274021	9.8344712	0.2297169	10.1139567	0.2320593	10.1552950	0.2401109	10.4234478	0.2405728	10.4710945
95	0.2847697	11.9041599	0.2319002	9.4777271	0.2338087	9.7346701	0.2366186	9.7901571	0.2445091	10.0467491	0.2449773	10.0939986
100	0.2873419	11.4077630	0.2343740	9.0757597	0.2358324	9.3099176	0.2390329	9.3747324	0.2467634	9.6208562	0.2472287	9.6666351
105	0.2880210	10.8842557	0.2386721	8.6500651	0.2379030	8.8520454	0.2407919	8.9226726	0.2473454	9.1617944	0.2478043	9.2060348
110	0.2874282	10.3619123	0.2446614	8.4727027	0.2435005	8.5176305	0.2467701	8.6071533	0.2496793	8.7163183	0.2495807	8.7358429
115	0.2861626	9.8615057	0.2493544	8.2673290	0.2478725	8.2998641	0.2514130	8.3935198	0.2543800	8.5034826	0.2542933	8.5167682
120	0.2844103	9.3895882	0.2526405	8.0375150	0.2509446	8.0621324	0.2546598	8.1557408	0.2577386	8.2653892	0.2576823	8.2792175
125	0.2824851	8.9483986	0.2544804	7.7830968	0.2526808	7.8039051	0.2564466	7.8936965	0.2596475	8.0033980	0.2596366	8.0179645

The ten-story structure model under seismic excitation was optimized with the AHS algorithm to obtain the minimum displacement. The optimized TLD parameters are given in Table 7.

Table 7. Optimum results for all TLD liquids in the 10-story structure.

Variables	Optimized Values				
	TLD				
	Chloroform	**Acetone**	**Propanol**	**Mercury**	**Seawater**
T_d (s)	1.0097	1.0301	0.9957	1.0201	0.9962
ζ_d	0.1843	0.2399	0.1839	0.2156	0.1841
R (m)	1.0416	0.9500	1.2055	0.3639	1.1087
h (m)	0.7641	10	0.8985	4.4510	0.7556

The critical earthquake record for the data obtained with the ten-story structure plus TLD optimization was the DUZCE/BOL090 earthquake. The maximum displacement and total acceleration values obtained from the critical seismic analysis are shown in Table 8.

Table 8. TLD + 10-story building model critical earthquake analysis results.

Liquid	Structure with TLD		Structure without TLD	
	Displacement (m)	**Total Acceleration (m/s^2)**	**Displacement (m)**	**Total Acceleration (m/s^2)**
Propanol	0.2971402	14.3139493	0.4101091	19.2833064
Seawater	0.2971696	14.3177283		
Chloroform	0.2974617	14.4231051		
Mercury	0.3017123	14.5490568		
Acetone	0.3070783	14.6519753		

The displacement–time and total acceleration–time graphs obtained from the critical earthquake analysis for propanol, seawater, chloroform, mercury, and acetone TLD liquids are shown in Figures 10–14, respectively.

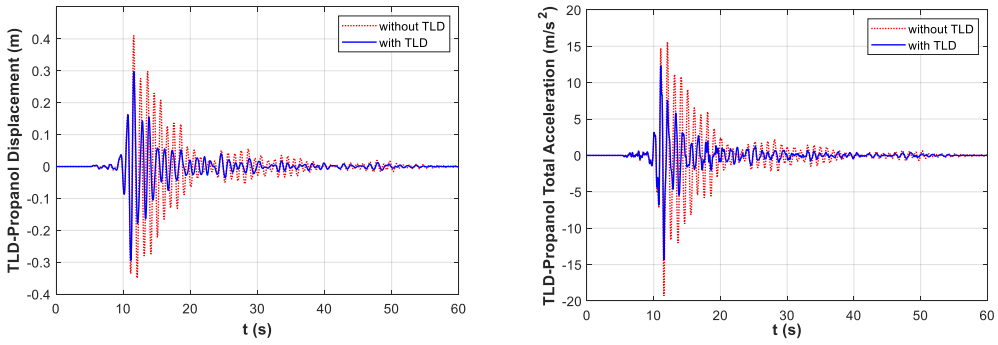

Figure 10. AHS optimization of the 10-story structure displacement–time and total acceleration–time graphs in the DUZCE/BOL090 earthquake record for TLD–propanol.

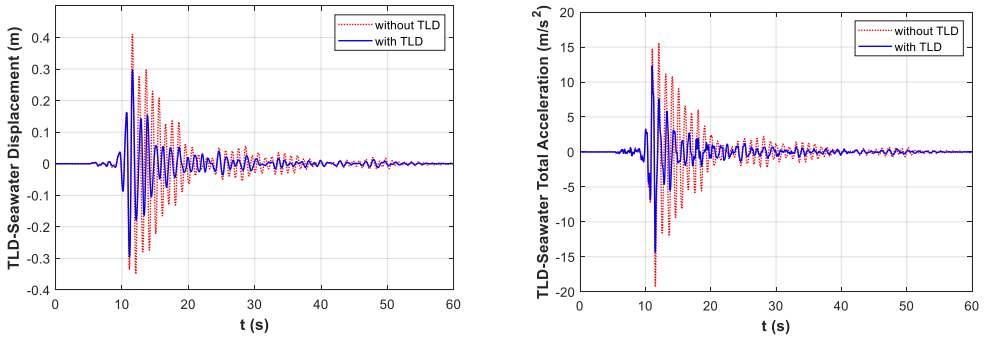

Figure 11. AHS optimization of the 10-story structure displacement–time and total acceleration–time graphs in the DUZCE/BOL090 earthquake record for TLD–seawater.

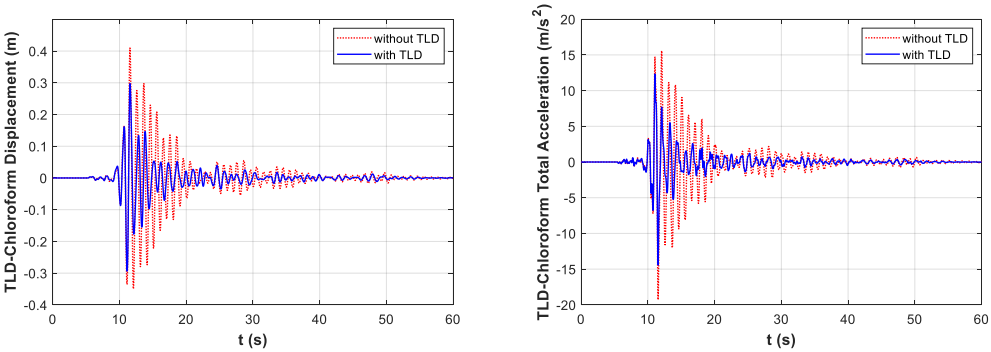

Figure 12. AHS optimization of the 10-story structure displacement–time and total acceleration–time graphs in the DUZCE/BOL090 earthquake record for TLD–chloroform.

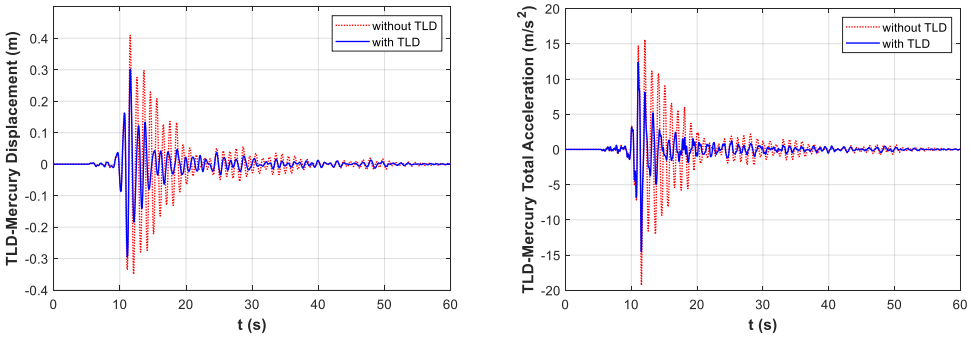

Figure 13. AHS optimization of the 10-story structure displacement–time and total acceleration–time graphs in the DUZCE/BOL090 earthquake record for TLD–mercury.

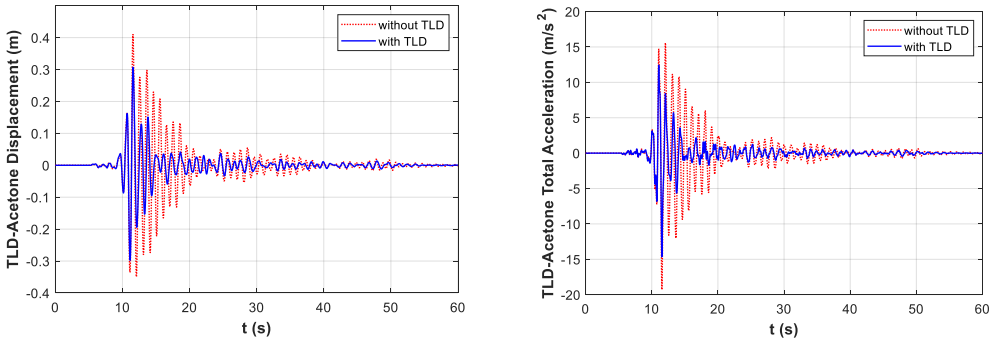

Figure 14. AHS optimization of the 10-story structure displacement–time and total acceleration–time graphs in the DUZCE/BOL090 earthquake record for TLD–acetone.

3.3. Forty-Story Structure

For the forty-story structure model, the structure with a floor mass of 980 tons was used. The stiffness and damping coefficient values of the forty-story structure were taken as 2130 MN/m and 42.6 MNs/m on the lowest floor and 998 MN/m and 20 MNs/m on the top floor. For the other stories, the coefficients were linearly changed [65]. The TLD + 40-story structure model designed with forty-two degrees of freedom (42DOF) is shown in 3D, and the idealized model is shown schematically in Figure 15.

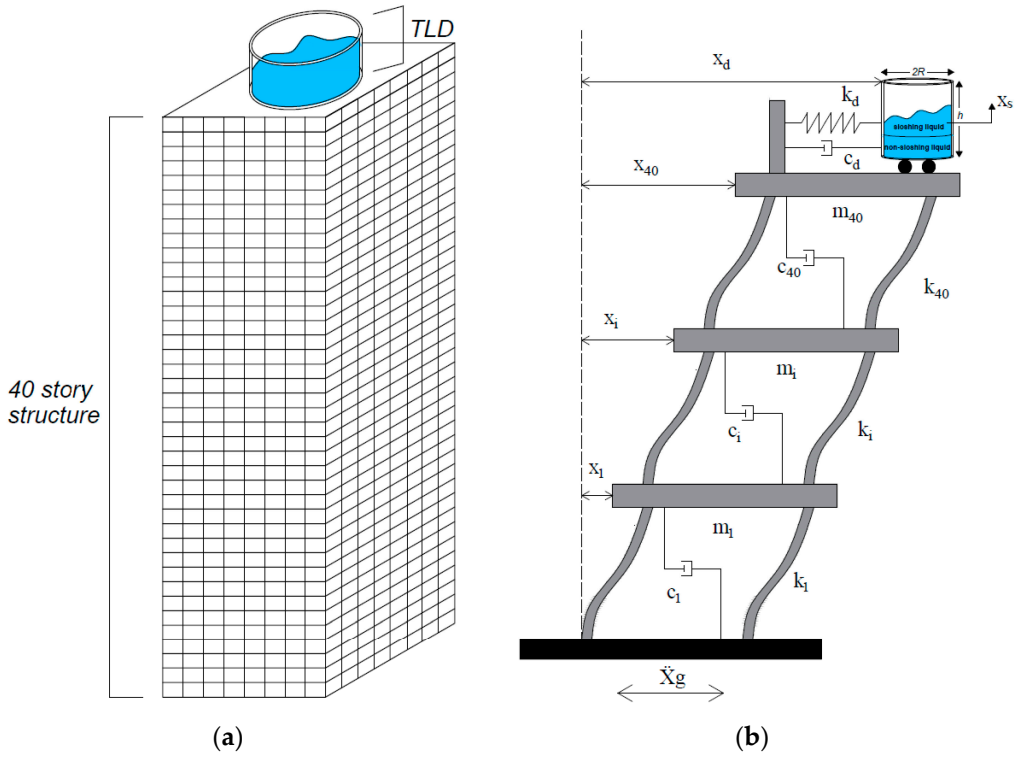

Figure 15. TLD + 40-story structure models: (**a**) 3D and (**b**) idealized model.

The obtained TLD design parameters of the forty-story structure model with the optimization process are shown in Table 9.

Table 9. Optimum results for all TLD liquids in the 40-story structure.

Variables	Optimized Values				
	TLD				
	Chloroform	**Acetone**	**Propanol**	**Mercury**	**Seawater**
T_d (s)	5.3564	5.0104	4.9877	3.5626	5.7453
ζ_d	0.1575	0.3991	0.3974	0.2270	0.1923
R (m)	5.7016	8.3976	8.3731	4.1312	5.9943
h (m)	7.3909	8.3196	8.0591	2.3684	7.6785

In the forty-story structure optimization, the critical earthquake record was the CHICHI/CHY101-N earthquake record in Chichi County, Taiwan. The maximum displacement and total acceleration values obtained from the critical seismic analysis are given in Table 10.

Table 10. TLD + 40-story building model critical seismic analysis results.

Liquid	Structure with TLD		Structure without TLD	
	Displacement (m)	**Total Acceleration (m/s^2)**	**Displacement (m)**	**Total Acceleration (m/s^2)**
Mercury	1.4018155	5.1254171	1.9277898	6.1734370
Chloroform	1.4226523	5.2496230		
Seawater	1.4570743	5.2789575		
Propanol	1.5225798	5.3138740		
Acetone	1.5234954	5.3147893		

The displacement–time and total acceleration–time graphs obtained from the critical seismic analysis for mercury, chloroform, seawater, propanol, and acetone TLD fluids are shown in Figures 16–20, respectively.

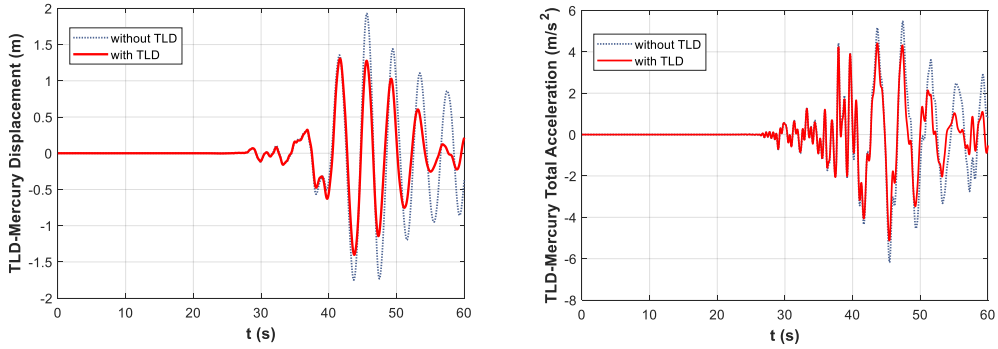

Figure 16. AHS optimization of the 40-story structure displacement–time and total acceleration–time graphs in the CHICHI/CHY101-N earthquake record for TLD–mercury.

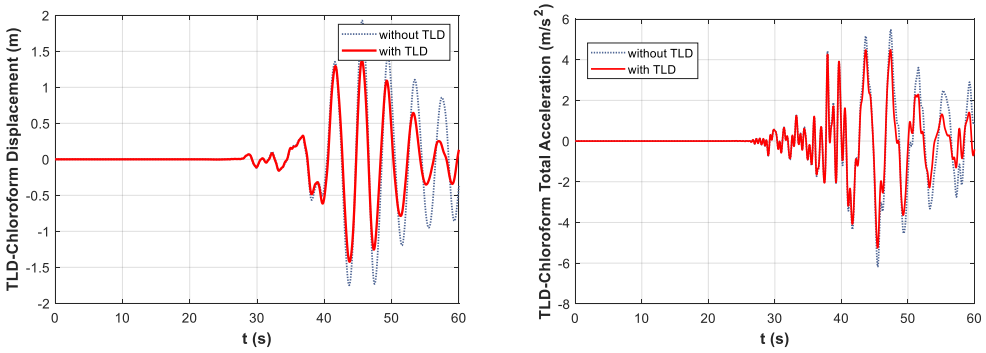

Figure 17. AHS optimization of the 40-story structure displacement–time and total acceleration–time graphs in the CHICHI/CHY101-N earthquake record for TLD–chloroform.

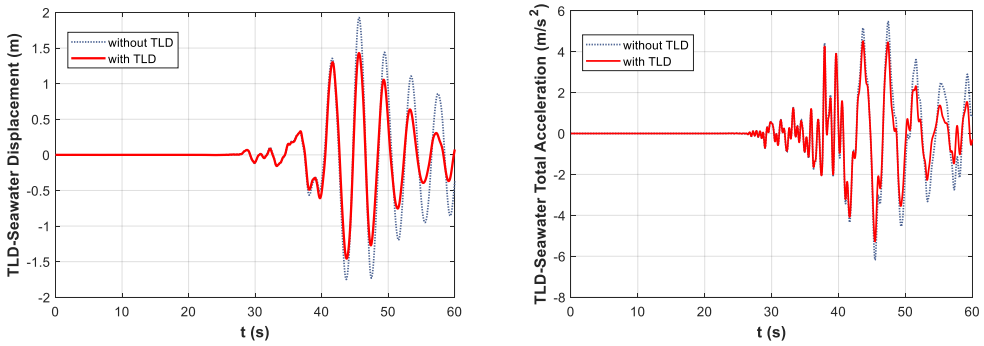

Figure 18. AHS optimization of the 40-story structure displacement–time and total acceleration–time graphs in the CHICHI/CHY101-N earthquake record for TLD–seawater.

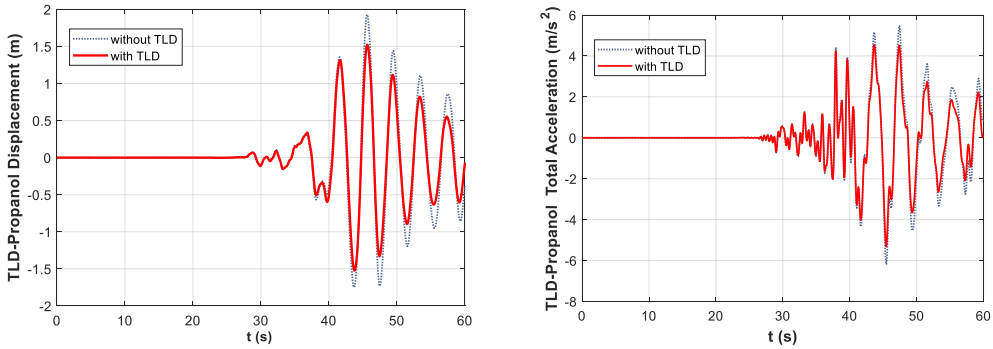

Figure 19. AHS optimization of the 40-story structure displacement–time and total acceleration–time graphs in the CHICHI/CHY101-N earthquake record for TLD–propanol.

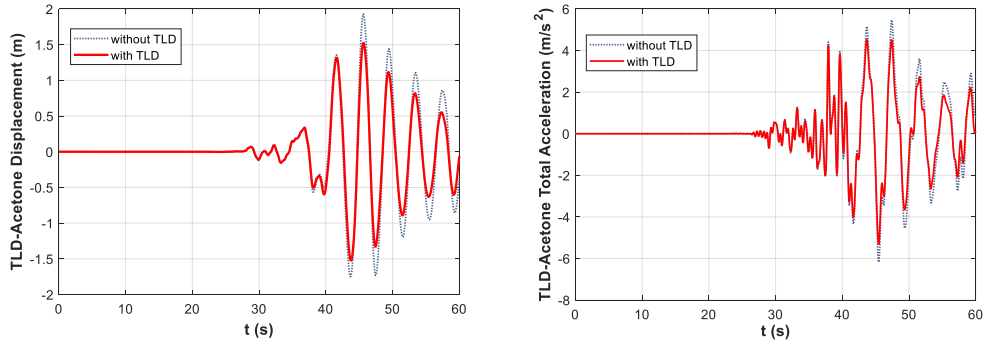

Figure 20. AHS optimization of the 40-story structure displacement–time and total acceleration–time graphs in the CHICHI/CHY101-N earthquake record for TLD–acetone.

4. Discussion

In this study, the effects of the characteristics of the liquids used in passively tuned TLD devices on the control performance were investigated. For this purpose, a type of TLD liquid with five different densities and viscosities was tested. Three structural models with 3 degrees of freedom (3DOF), 12 degrees of freedom (12DOF), and 42 degrees of freedom (42DOF) for a single-story, ten-story, and forty story structure, respectively, were created to evaluate the TLD damping performance. FEMA earthquake records consisting of 22 two-component earthquake records were sent to the selected models as excitation, and the TLD parameters were optimized with an AHS algorithm to minimize the movements of the structures. In the critical earthquake record obtained from the optimization, the displacement and total acceleration drop percentages obtained from the analysis of all TLD liquids for the single-story structure model are shown in Table 11.

Table 11. Structure displacement and total acceleration reduction percentages with TLD for a single-story structure.

Variable	Single-Story Structure		Kinematic Viscosity (m^2/s)	Density (kg/m^3)
	Displacement (%)	Total Acceleration (%)		
Acetone	18.43	20.44	3.90×10^{-7}	784.89
Mercury	17.92	18.39	1.15×10^{-7}	13600
Chloroform	16.81	17.82	3.92×10^{-7}	1480.3
Propanol	14.12	15.66	2.43×10^{-6}	799.60
Sea water	13.96	15.26	1.17×10^{-6}	1030

According to the data in Table 11, the optimum displacement reduction percentage for the single-story structure model was obtained when acetone liquid was used. It had very close reduction percentages with mercury, which was the optimum second liquid. When the density and kinematic viscosities of the first three optimum liquids were examined, it was seen that the kinematic viscosities were the smallest among the five liquids. From this point of view, it is understood that it may be advantageous to have a small kinematic viscosity. Of the top three liquids in the ranking, acetone and chloroform had nearly the same kinematic viscosity, with chloroform twice as dense as acetone. Therefore, it can be said that, in liquids with similar kinematic viscosity properties, the less dense liquid moved closer to the optimum result. When compared according to density, mercury, which is ten times denser than other liquids, ranks second, explaining that density is insufficient to be a determining criterion for a single-story structure, and viscosity is more prominent.

The displacement and total acceleration reduction percentages of the critical seismic analysis obtained from the ten-story structure model optimization are given in Table 12.

Table 12. Structure displacement and total acceleration reduction percentages with TLD for the 10-story structure.

Variable	10-Story Structure		Kinematic Viscosity (m^2/s)	Density (kg/m^3)
	Displacement (%)	Total Acceleration (%)		
Propanol	27.55	25.77	2.43×10^{-6}	799.60
Sea water	27.54	25.75	1.17×10^{-6}	1030
Chloroform	27.47	25.20	3.92×10^{-7}	1480.3
Mercury	26.43	24.55	1.15×10^{-7}	13600
Acetone	25.12	24.02	3.90×10^{-7}	784.89

In light of the information given in Table 12, it is seen that the optimum liquid is propanol. In the ten-story structure, unlike the single-story structure, it is seen that the liquids with the highest viscosity are in the first two places in reducing displacement. It can be said that the increase in the number of floors and, therefore, the mass of the structure creates a greater need for viscosity in terms of performance compared to the single-story structure. Looking at the last three liquids in the table, it is understood that the denser one is more efficient than chloroform and acetone, whose kinematic viscosities are very close. In light of this information, it shows that the choice of a more viscous liquid will increase the efficiency, with a little increase in the structure mass.

The displacement and total acceleration reduction percentages of the critical seismic analysis for the forty-story structure are shown in Table 13.

Table 13. Structure displacement and total acceleration reduction percentages with TLD for the 40-story structure.

Variable	40-Story Structure		Kinematic Viscosity (m^2/s)	Density (kg/m^3)
	Displacement (%)	Total Acceleration (%)		
Mercury	27.28	16.98	1.15×10^{-7}	13600
Chloroform	26.20	14.96	3.92×10^{-7}	1480.3
Sea water	24.42	14.49	1.17×10^{-6}	1030
Propanol	21.02	13.92	2.43×10^{-6}	799.60
Acetone	20.97	13.91	3.90×10^{-7}	784.89

When Table 13 is examined, it is seen that the liquids in the first row are less densely viscous liquids. Acetone breaks this harmony. In the table, the optimum liquid is seen in mercury with a very low viscosity, as well as being the densest. Acetone, despite having a small viscosity, took the last place in the ranking. Chloroform liquid with a similar viscosity was in second place with a decrease of 26%, while acetone was in the last place. This may be because it had almost half the density of chloroform. In addition, acetone provided almost the same percentage reduction as propanol, which was very similar in density. According to the density and viscosity relationship between them, more viscous propanol came to the fore. Considering all these situations, it was seen that, unlike the ten-story structure, as the mass of the structure increased, the density came to the fore, and the denser liquid performed better. It may not be correct to make this generalization for viscosity.

When Tables 11–13 are examined, rates of 18.43% and 20.44% in the single-story structure, 27.55% and 25.77% in the ten-story structure, and 27.28% and 16.98% in the forty-story structure, respectively, were obtained in reducing the displacement and total acceleration with TLD optimization. Optimization with the AHS algorithm made the TLDs more efficient, resulting in good antivibration. According to all liquid analyses, it was seen that it is an effective method in reducing not only the displacement but also the total acceleration.

5. Conclusions

The following results were obtained with the optimization of the TLDs.

- The ideal liquid for a single-story structure is acetone. According to the liquid analysis, it has been observed that choosing a TLD liquid with a smaller viscosity to be used for a single-story normal weight structure will increase the efficiency, while a less dense liquid with similar viscosity liquids will increase the performance.
- It can be said that, in the ten-story structure design, since the structure mass increases compared to the single-story structure, the low viscosity required in the design is replaced by a more viscous liquid. It has been understood that the performance of the more viscous liquid increases with a slight increase in the mass, and in contrast to the single-story structure in the liquid with similar viscosity, the one with the higher density is more efficient. Increasing the structure mass a little bit brought the viscosity to the fore.
- For the forty-story heavy structure, the optimum liquid was mercury, which is the densest. It is seen that continuing to increase the structure mass compared to the ten-story structure is related to density in terms of efficiency. Although a precise comparison of the viscosity cannot be made for heavy structures, it has been observed that a denser liquid should be preferred.
- As a result of all the liquid analyses, it is understood that remarkable displacement and total acceleration decreases will be achieved with the optimization of the TLDs.
- For vibration control, the best factor for the success of the method is to use the most realistic model in the dynamic analysis. In that case, soil–structure interactions (SSIs)

can play an important role in the optimum design of control systems. In the last decade, the SSI effect has been considered in several studies related to tuned mass dampers [65–69]. As a future work, the SSI effect can be also considered in the optimization of TLDs.

- In the design of structures, the variable loads are assumed as the standard values. In that case, the mass of structures is uncertain, and it may change the frequency content of the system. Due to that, the optimum parameters are affected, and the control systems may be not effective in that case. In the present study, the single-story structure cases were investigated for different mass values for the optimum TLD parameters that were found for the assumed mass. While the best performance was seen for acetone with 18.43% and 20.38% reduction of displacement and acceleration, respectively, the response reductions reduced to 18.27% and 19.17% for the 25% reduction of the mass. These reductions were small, and the optimum TLD was also effective for the mass increase, but the values for displacement and acceleration, respectively, reduced 9.91% and 13.02% due to the reduction of the mass ratio of the TLD and structure. In general, the TLD was proven as a robust system. In future works, a multi-objective approach that considers the response of several possible structure properties can be developed.
- In structural control systems, it is important to test failure situations with experimental simulations [70]. This is also valid for TLDs, and it can be considered in future works.

In light of all these data, it has been determined that the optimization of TLDs improves the performance, and the choice of liquid to be used is related to the structure mass.

Author Contributions: A.O., G.B. and S.M.N. generated the analysis code. A.O. and S.M.N. developed the theoretical background and formulations of the passive control system. The modification of HS was done by A.O. and G.B. The text of the paper was written by S.M.N., G.B. and A.O. The figures were drawn by S.M.N., G.B. and A.O., S.K. and Z.W.G. edited the paper and supervised the research direction. All authors have read and agreed to the published version of the manuscript.

Funding: This research was supported by the Energy Cloud R&D Program through the National Research Foundation of Korea (NRF) funded by the Ministry of Science, ICT (2019M3F2A1073164).

Institutional Review Board Statement: Not applicable.

Informed Consent Statement: Not applicable.

Data Availability Statement: The data of the paper can be requested via e-mail to corresponding author.

Conflicts of Interest: The authors declare no conflict of interest.

Nomenclature

Symbols and Abbreviations	Description
3DOF	Three degrees of freedom
12DOF	Twelve degrees of freedom
42DOF	Forty-two degrees of freedom
AHS	Adaptive harmony search algorithm
C	Damping coefficient matrix
c	Damping coefficient
c_d	TLD damping coefficient
c_s	Damping coefficient of sloshing liquid
FEMA	Quantification of Building Seismic Performance Factors
FW	Fret width
FW_{in}	Initial Fret Width
g	Gravitational acceleration
h	Liquid height in the TLD tank

HMCR	Harmony Memory Consideration Rate
$HMCR_{in}$	Initial Harmony Memory Consideration Rate
HMS	Harmony memory size
HS	Harmony Search Algorithm
K	Stiffness matrix
k	Structure stiffness coefficient
k_s	Sloshing liquid stiffness
k_d	TLD stiffness
LCVA	Liquid column vibration absorbers
M	Mass matrix
m	Mass of structure
m_d	Empty tank mass and passive liquid mass of TLD
MR	Magneto rheological
m_s	Mass of sloshing liquid
m_{st}	Total liquid mass
mt	maximum iteration number
MTLCD	Multiple Tuned Liquid Column Damper
MTLCDI	Multiple tuned liquid column damper inerter
m_{TLD}	Mass of TLD
R	Tank radius of TLD
$Stmax$	Stroke capacity
s	Second
t	Iteration number
T_d	Period of TLD
TLCBD	Tuned liquid column ball damper
TLCBSD	Tuned liquid column ball spring damper
TLCD	Tuned liquid column damper
TLCDI	Tuned liquid column damper inerter
TLD	Tuned liquid damper
TMD	Tuned mass damper
x	Horizontal displacement of the structure relative to the ground
X_{max}	Upper limit for design variable
X_{min}	Lower limit for design variable
X_n	n^{th} Harmony
X_{new}	New value in design
$\dot{X}$	Velocity of structure
$\ddot{X}$	Acceleration of structure
$\ddot{X}_g$	Acceleration of ground
ζ_d	Damping rate of TLD
ζ_s	Damping rate of sloshing liquid
ξ_{mn}	The damping ratio of the liquid according to the vibration mode in the tangential (m) and radial (n) directions
v	Kinematic viscosity
ρ	Density of liquid

References

1. Abramson, H.N. *The Dynamic Behavior of Liquids in Moving Containers*; NASA SP-106; NASA Special Publication: Washington, DC, USA, 1966; Volume 106.
2. Ibrahim, R.A. *Liquid Sloshing Dynamics: Theory and Applications*; Cambridge University Press: Cambridge, UK, 2005; ISBN 0-521-83885-1.
3. Sun, L.M.; Fujino, Y.; Pacheco, B.M.; Chaiseri, P. Modeling of tuned liquid damper (TLD). *J. Wind. Eng. Ind. Aerodyn.* **1992**, *43*, 1883–1894. [CrossRef]
4. Yu, J.K.; Wakahara, T.; Reed, D.A. A non-linear numerical model of the tuned liquid damper. *Earthq. Eng. Struct. Dyn.* **1999**, *28*, 671–686. [CrossRef]
5. Vickery, B.J.; Isyumov, N.; Davenport, A.G. The role of dumping, mass, and acceleration. *J. Wind Eng. Ind. Aerodyn.* **1983**, *11*, 285–294. [CrossRef]
6. Rana, R.; Soong, T.T. Parametric study and simplified design of tuned mass dampers. *Eng. Struct.* **1998**, *20*, 193–204. [CrossRef]

7. Wang, Q.; Tiwari, N.D.; Qiao, H.; Wang, Q. Inerter-based tuned liquid column damper for seismic vibration control of a single-degree-of-freedom structure. *Int. J. Mech. Sci.* **2020**, *184*, 105840. [CrossRef]
8. Di Matteo, A.; Masnata, C.; Adam, C.; Pirrotta, A. Optimal design of tuned liquid column damper inerter for vibration control. *Mech. Syst. Signal Process.* **2022**, *167*, 108553. [CrossRef]
9. Wang, Q.; Qiao, H.; De Domenico, D.; Zhu, Z.; Tang, Y. Seismic performance of optimal Multi-Tuned Liquid Column Damper-Inerter (MTLCDI) applied to adjacent high-rise buildings. *Soil Dyn. Earthq. Eng.* **2021**, *143*, 106653. [CrossRef]
10. Chang, C.C.; Gu, M. Suppression of vortex-excited vibration of tall buildings using tuned liquid dampers. *J. Wind. Eng. Ind. Aerodyn.* **1999**, *83*, 225–237. [CrossRef]
11. Casciati, F.; De Stefano, A.; Matta, E. Simulating a conical tuned liquid damper. *Simul. Model. Pract. Theory* **2003**, *11*, 353–370. [CrossRef]
12. Zhang, Z. Numerical and experimental investigations of the sloshing modal properties of sloped-bottom tuned liquid dampers for structural vibration control. *Eng. Struct.* **2020**, *204*, 110042. [CrossRef]
13. Cavalagli, N.; Agresta, A.; Biscarini, C.; Ubertini, F.; Ubertini, S. Enhanced energy dissipation through 3D printed bottom geometry in Tuned Sloshing Dampers. *J. Fluids Struct.* **2021**, *106*, 103377. [CrossRef]
14. Fujino, Y.; Sun, L.; Pacheco, B.M.; Chaiseri, P. Tuned liquid damper (TLD) for suppressing horizontal motion of structures. *J. Eng. Mech.* **1992**, *118*, 2017–2030. [CrossRef]
15. Balendra, T.; Wang, C.M.; Cheong, H.F. Effectiveness of tuned liquid column dampers for vibration control of towers. *Eng. Struct.* **1995**, *17*, 668–675. [CrossRef]
16. Ocak, A.; Bekdaş, G.; Nigdeli, S.M. A metaheuristic-based optimum tuning approach for tuned liquid dampers for structures. *Struct. Des. Tall Spec. Build.* **2022**, *31*, e1907. [CrossRef]
17. Tanveer, M.; Usman, M.; Khan, I.U.; Farooq, S.H.; Hanif, A. Material optimization of tuned liquid column ball damper (TLCBD) for the vibration control of multi-story structures using various liquid and ball densities. *J. Build. Eng.* **2020**, *32*, 101742. [CrossRef]
18. Shah, M.U.; Usman, M.; Farooq, S.H.; Kim, I.H. Effect of Tuned Spring on Vibration Control Performance of Modified Liquid Column Ball Damper. *Appl. Sci.* **2022**, *12*, 318. [CrossRef]
19. Hitchcock, P.A.; Kwok, K.C.S.; Watkins, R.D.; Samali, B. Characteristics of liquid column vibration absorbers (LCVA)—I. *Eng. Struct.* **1997**, *19*, 126–134. [CrossRef]
20. Xin, Y.; Chen, G.; Lou, M. Seismic response control with density-variable tuned liquid dampers. *Earthq. Eng. Eng. Vib.* **2009**, *8*, 537–546. [CrossRef]
21. Debbarma, R.; Chakraborty, S.; Ghosh, S.K. Optimum design of tuned liquid column dampers under stochastic earthquake load considering uncertain bounded system parameters. *Int. J. Mech. Sci.* **2010**, *52*, 1385–1393. [CrossRef]
22. Das, S.; Choudhury, S. Seismic response control by tuned liquid dampers for low-rise RC frame buildings. *Aust. J. Struct. Eng.* **2017**, *18*, 135–145. [CrossRef]
23. Sun, H.; Wang, X.; Chen, Z. Magnetorheological tuned liquid column damper (MR-TLCD) for semi-active control of structures under earthquake. *J. Earthq. Eng. Eng. Vib.* **2010**, *30*, 22–28.
24. Cheng, C.W.; Lee, H.H.; Luo, Y.T. Experimental study of controllable MR-TLCD applied to the mitigation of structure vibration. *Smart Struct. Syst.* **2015**, *15*, 1481–1501. [CrossRef]
25. Xin, C.; Aiqun, L.; Zhiqiang, Z. Optimum design of ring-shape TLD control for high-rise structure using multi-objective genetic algorithm. *China Civ. Eng. J.* **2014**, *47*, 73–81.
26. Ab Talib, M.H.; Darus, I.Z.M. Fuzzy logic with firefly algorithm for semi-active suspension system using a magneto-rheological damper. In Proceedings of the 2014 IEEE Symposium on Industrial Electronics & Applications (ISIEA), Kota Kinabalu, Malaysia, 28 September–1 October 2014; pp. 142–147.
27. Mohebbi, M.; Dabbagh, H.R.; Shakeri, K. Optimal design of multiple tuned liquid column dampers for seismic vibration control of MDOF structures. *Period. Polytech. Civ. Eng.* **2015**, *59*, 543–558. [CrossRef]
28. Xin, C.; Ai-qun, L.I.; Qing-yang, X.U.; Zhi-Qiang, Z.H.A.N.G. Satisfaction optimum design of ring-shaped tld control for high-rise structure using genetic algorithm. *Eng. Mech.* **2016**, *33*, 77–84.
29. Abubaker, S.; Nagan, S.; Nasar, T. Particle swarm optimized fuzzy control of structure with tuned liquid column damper. *Glob. J. Pure Appl. Math.* **2016**, *12*, 875–886.
30. Ab Talib, M.H.; Mat Darus, I.Z. Intelligent fuzzy logic with firefly algorithm and particle swarm optimization for semi-active suspension system using a magneto-rheological damper. *J. Vib. Control* **2017**, *23*, 501–514. [CrossRef]
31. Samiee, H.R. The hybrid passive control system of TLD and TMD for seismic response mitigation of Tall Buildings. *J. Vibroeng.* **2017**, *19*, 3648–3667. [CrossRef]
32. Das, S.; Chakraborty, A. Optimal Design of MRTLCD for Semi-active Vibration Control of Building Structures Using Genetic Algorithm. In *Advances in Rotor Dynamics, Control, and Structural Health Monitoring*; Springer: Singapore, 2020; pp. 615–625.
33. Geem, Z.W.; Kim, J.H.; Loganathan, G.V. A new heuristic optimization algorithm: Harmony search. *Simulation* **2001**, *76*, 60–68. [CrossRef]
34. Nigdeli, S.M.; Bekdas, G.; Kim, S.; Geem, Z.W. A novel harmony search-based optimization of reinforced concrete biaxially loaded columns. *Struct. Eng. Mech. Int. J.* **2015**, *54*, 1097–1109. [CrossRef]
35. Siddique, N.; Adeli, H. Applications of harmony search algorithms in engineering. *Int. J. Artif. Intell. Tools* **2015**, *24*, 1530002. [CrossRef]

36. De Almeida, F.S. Optimization of laminated composite structures using a harmony search algorithm. *Compos. Struct.* **2019**, *221*, 110852. [CrossRef]
37. Cakiroglu, C.; Bekdaş, G.; Kim, S.; Geem, Z.W. Optimization of Shear and Lateral–Torsional Buckling of Steel Plate Girders Using Meta-Heuristic Algorithms. *Appl. Sci.* **2020**, *10*, 3639. [CrossRef]
38. Cakiroglu, C.; Islam, K.; Bekdaş, G.; Kim, S.; Geem, Z.W. Metaheuristic Optimization of Laminated Composite Plates with Cut-Outs. *Coatings* **2021**, *11*, 1235. [CrossRef]
39. Kayabekir, A.E.; Bekdaş, G.; Nigdeli, S.M.; Geem, Z.W. Optimum design of PID controlled active tuned mass damper via modified harmony search. *Appl. Sci.* **2020**, *10*, 2976. [CrossRef]
40. Ulusoy, S.; Bekdaş, G.; Nigdeli, S.M.; Kim, S.; Geem, Z.W. Performance of optimum tuned PID controller with different feedback strategies on active-controlled structures. *Appl. Sci.* **2021**, *11*, 1682. [CrossRef]
41. Nigdeli, S.M.; Bekdaş, G. Optimum tuned mass damper design in the frequency domain for structures. *KSCE J. Civ. Eng.* **2017**, *21*, 912–922. [CrossRef]
42. Jin, C.; Chung, W.C.; Kwon, D.S.; Kim, M. Optimization of tuned mass damper for seismic control of submerged floating tunnel. *Eng. Struct.* **2021**, *241*, 112460. [CrossRef]
43. Zhang, H.Y.; Zhang, L.J. Tuned mass damper system of high-rise intake towers optimized by the improved harmony search algorithm. *Eng. Struct.* **2017**, *138*, 270–282. [CrossRef]
44. Den Hartog, J.P. *Mechanical Vibrations*, 3rd ed.; McGraw-Hill: New York, NY, USA, 1947; ISBN 978-1443725361.
45. Warburton, G.B. Optimum absorber parameters for various combinations of response and excitation parameters. *Earthq. Eng. Struct. Dyn.* **1982**, *10*, 381–401. [CrossRef]
46. Sadek, F.; Mohraz, B.; Taylor, A.W.; Chung, R.M. A method of estimating the parameters of tuned mass dampers for seismic application. *Earthq. Eng. Struct. Dyn.* **1997**, *26*, 617–635. [CrossRef]
47. Leung, A.Y.T.; Zhang, H. Particle swarm optimization of tuned mass dampers. *Eng. Struct.* **2009**, *31*, 715–728. [CrossRef]
48. Keshtegar, B.; Etedali, S. Nonlinear mathematical modeling and optimum design of tuned mass dampers using adaptive dynamic harmony search algorithm. *Struct. Control Health Monit.* **2018**, *25*, e2163. [CrossRef]
49. Alkhadashi, A.; Mohammad, F.; Zubayr, R.O.; Klalib, H.A.; Balik, P. Multi-objective design optimization of steel-framed structures using three different methods. *Int. J. Struct. Integr.* **2021**, *13*, 92–111. [CrossRef]
50. Toklu, Y.C.; Bekdaş, G.; Yücel, M.; Nigdeli, S.M.; Kayabekir, A.E.; Kim, S.; Geem, Z.W. Total Potential Optimization Using Metaheuristic Algorithms for Solving Nonlinear Plane Strain Systems. *Appl. Sci.* **2021**, *11*, 3220. [CrossRef]
51. Keshtegar, B.; Nehdi, M.L.; Kolahchi, R.; Trung, N.T.; Bagheri, M. Novel hybrid machine learning model for predicting the shear strength of reinforced concrete shear walls. *Eng. Comput.* **2021**, 1–12. [CrossRef]
52. Peifeng, W.; Liqun, G.; Xiang, Z.; Dongli, Z. Application of adaptive harmony search algorithm in Structural engineering design. *Chin. J. Sci. Instrum.* **2012**, *33*, 1676–1680.
53. Ocak, A.; Nigdeli, S.M.; Bekdaş, G.; Kim, S.; Geem, Z.W. Adaptive Harmony Search for Tuned Liquid Damper Optimization under Seismic Excitation. *Appl. Sci.* **2022**, *12*, 2645. [CrossRef]
54. The MathWorks. *Matlab R2018a*; The MathWorks: Natick, MA, USA, 2018.
55. FEMA P-695. *Quantification of Building Seismic Performance Factors*; FEMA: Washington, DC, USA, 2008.
56. Sharma, V.; Arun, C.O.; Krishna, I.P. Development and validation of a simple two degree of freedom model for predicting maximum fundamental sloshing mode wave height in a cylindrical tank. *J. Sound Vib.* **2019**, *461*, 114906. [CrossRef]
57. Bauer, H.F. Tables, and graphs of zeros of cross-product Bessel functions. *Math. Comput.* **1964**, *18*, 128.
58. Mikishev, G.N.; Dorozhkin, N.Y. An experimental investigation of free oscillations of a liquid in containers. *Izv. Akad. Nauk. SSSR Otd. Tekhnicheskikh Nauk. Mekhanika Mashinostroenie* **1961**, *4*, 48–53.
59. Lide, D.R. *CRC Handbook of Chemistry and Physics*; CRC Press: Boca Raton, FL, USA, 2004; Volume 85.
60. Munson, R.B.; Young, D.F.; Okiishi, T.H. *Fundamentals of Fluid Mechanics*, 2nd ed.; John Wiley & Sons, Inc.: Hoboken, NJ, USA, 1995.
61. Istanbul University. Available online: https://avesis.istanbul.edu.tr/resume/downloadfile/emine.kahraman?key=e3a09eb3-c53f-4e2f-a64a-32849279de25 (accessed on 3 March 2022).
62. Atik, Z. Densities and excess molar volumes of binary and ternary mixtures of aqueous solutions of 2, 2, 2-trifluoroethanol with acetone and alcohols at the temperature of 298.15 K and Pressure of 101 kPa. *J. Solut. Chem.* **2004**, *33*, 1447–1466. [CrossRef]
63. El-Hammamy, N.H.; El-Kholy, M.M.; Amira, M.F. Effect of the dielectric constant of the medium on conductance for acetylcholine halides and perchlorate in normal and branched alcohols. *J. Indian Chem. Soc.* **2008**, *85*, 1112.
64. Singh, M.P.; Singh, S.; Moreschi, L.M. Tuned mass dampers for response control of torsional buildings. *Earthq. Eng. Struct. D.* **2002**, *31*, 749–769. [CrossRef]
65. Liu, M.Y.; Chiang, W.L.; Hwang, J.H.; Chu, C.R. Wind-induced vibration of high-rise building with tuned mass damper including soil–structure interaction. *J. Wind. Eng. Ind. Aerodyn.* **2008**, *96*, 1092–1102. [CrossRef]
66. Bekdaş, G.; Kayabekir, A.E.; Nigdeli, S.M.; Toklu, Y.C. Tranfer function amplitude minimization for structures with tuned mass dampers considering soil-structure interaction. *Soil Dyn. Earthq. Eng.* **2019**, *116*, 552–562. [CrossRef]
67. Bekdaş, G.; Nigdeli, S.M. Metaheuristic based optimization of tuned mass dampers under earthquake excitation by considering soil-structure interaction. *Soil Dyn. Earthq. Eng.* **2017**, *92*, 443–461. [CrossRef]

68. Liu, S.; Lu, Z.; Li, P.; Zhang, W.; Taciroglu, E. Effectiveness of particle tuned mass damper devices for pile-supported multi-story frames under seismic excitations. *Struct. Control Health Monit.* **2020**, *27*, e2627. [CrossRef]
69. Zhang, W.; Liu, S.; Shokrabadi, M.; Dehghanpoor, A.; Taciroglu, E. Nonlinear seismic fragility assessment of tall buildings equipped with tuned mass damper (TMD) and considering soil-structure interaction effects. *Bull. Earthq. Eng.* **2022**, 1–15. [CrossRef]
70. Guan, D.; Jing, X.; Shen, H.; Jing, L.; Gong, J. Test and simulation the failure characteristics of twin tube shock absorber. *Mech. Syst. Signal Process.* **2019**, *122*, 707–719. [CrossRef]